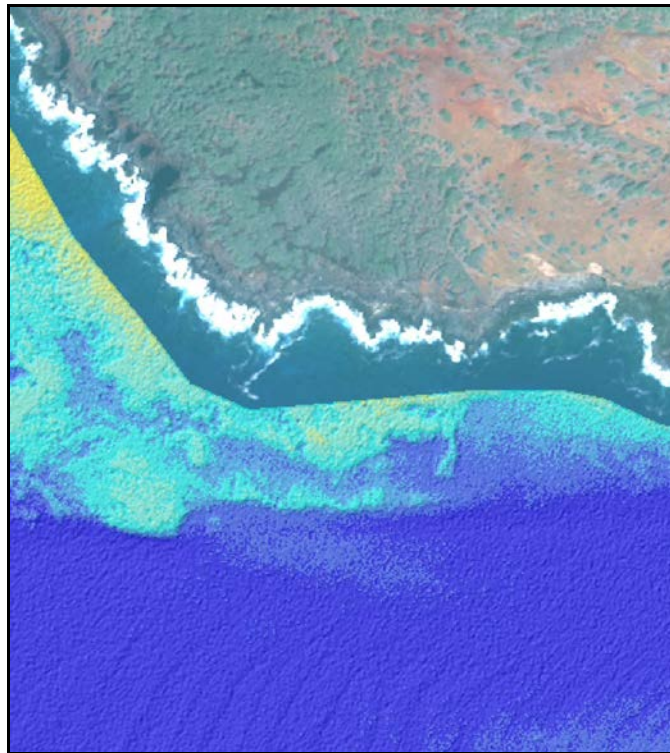# Depth Derivation Using Multispectral WorldView-2 Satellite Imagery

Julia S. Ehses
John J. Rooney

Pacific Islands Fisheries Science Center
National Marine Fisheries Service
National Oceanic and Atmospheric Administration
U.S. Department of Commerce

About this document

The mission of the National Oceanic and Atmospheric Administration (NOAA) is to understand and predict changes in the Earth's environment and to conserve and manage coastal and oceanic marine resources and habitats to help meet our Nation's economic, social, and environmental needs. As a branch of NOAA, the National Marine Fisheries Service (NMFS) conducts or sponsors research and monitoring programs to improve the scientific basis for conservation and management decisions. NMFS strives to make information about the purpose, methods, and results of its scientific studies widely available.

NMFS' Pacific Islands Fisheries Science Center (PIFSC) uses the **NOAA Technical Memorandum NMFS** series to achieve timely dissemination of scientific and technical information that is of high quality but inappropriate for publication in the formal peer-reviewed literature. The contents are of broad scope, including technical workshop proceedings, large data compilations, status reports and reviews, lengthy scientific or statistical monographs, and more. NOAA Technical Memoranda published by the PIFSC, although informal, are subjected to extensive review and editing and reflect sound professional work. Accordingly, they may be referenced in the formal scientific and technical literature.

A **NOAA Technical Memorandum NMFS** issued by the PIFSC may be cited using the following format:

> Ehses, J. S., and J. J. Rooney.
>> 2015. Depth derivation using multispectral WorldView-2 satellite imagery. U.S. Dep. Commer., NOAA Tech. Memo., NOAA-TM-NMFS-PIFSC-46, 24 p.
>> doi:10.7289/V5668B40

────────────────────────────

For further information direct inquiries to

──

Cover: Multispectral WorldView-2 imagery and derived depths of the south shore of Niihau island, main Hawaiian Islands.

Pacific Islands Fisheries Science Center
National Marine Fisheries Service
National Oceanic and Atmospheric Administration
U.S. Department of Commerce

Depth Derivation using Multispectral WorldView-2 Satellite Imagery

[1]Julia S. Ehses
[2]John J. Rooney

[1]Joint Institute for Marine and Atmospheric Research
University of Hawaii
1000 Pope Road
Honolulu, Hawaii 96822

[2]Pacific Islands Fisheries Science Center
National Marine Fisheries Service
1845 Wasp Boulevard
Building 176
Honolulu, Hawaii 96818

ABSTRACT

Despite recent efforts to collect high-resolution multibeam bathymetry data across the Pacific Islands Region, significant gaps exist in the 0–30 m depth range. Achieving bathymetric coverage in these areas is critical for assessing the health of coral reef ecosystems that reside there. Here we use WorldView-2 multispectral satellite imagery and two depth derivation methods (Lyzenga, 2006; Stumpf et al., 2003) that relate spectral radiance values to ground truth depth information to derive depths for shallow-water regions in the main Hawaiian Islands. Our results show increased accuracy using the Lyzenga (2006) multiple linear regression method when compared to the Stumpf et al. (2003) ratio method. Furthermore, we achieved improved results by eliminating the linearization process from the Lyzenga (2006) method. This improvement may be related to the lack of large seagrass aggregations within the main Hawaiian Islands because the presence of seagrass has been shown to affect the linear relationship between ground truth depth and spectral radiance values (Doxani et al., 2012). The accuracy of our derived depth product is directly related to the quality of the multispectral satellite images, the availability of ground truth data, and water depth with accuracy decreasing substantially in water depths > 20 m. Our results show that in the absence of shallow (0–20 m) high-resolution bathymetric data, satellite-derived depths are an important resource for assessing, monitoring, and managing shallow coral reef ecosystems.

CONTENTS

LIST OF FIGURES

LIST OF TABLES

LIST OF ABBREVIATIONS

CRED	Coral Reef Ecosystem Division
DN	Digital Number
EM	Electromagnetic
ENC	Electronic Navigational Chart
LiDAR	Light Detection and Ranging
MHI	main Hawaiian Islands
NIR	Near-infrared
NOAA	National Oceanic and Atmospheric Administration
REA	Rapid Ecological Assessment
TOA	Top-of-atmosphere
WV-2	WorldView-2

x

INTRODUCTION

As part of the National Oceanic and Atmospheric Administration (NOAA) Coral Reef Conservation Program, primary objectives of the NOAA Pacific Islands Fisheries Science Center's Coral Reef Ecosystem Division (CRED) are to monitor, map, and understand coral reef ecosystems to inform resource management and support conservation activities and decision making across the Pacific Islands Region (Fig. 1). CRED's benthic habitat mapping produces maps of habitat characteristics, including bathymetry and coral cover. These products provide a scientific basis for spatial planning and management and are essential tools for gaining a better understanding of marine ecosystems.
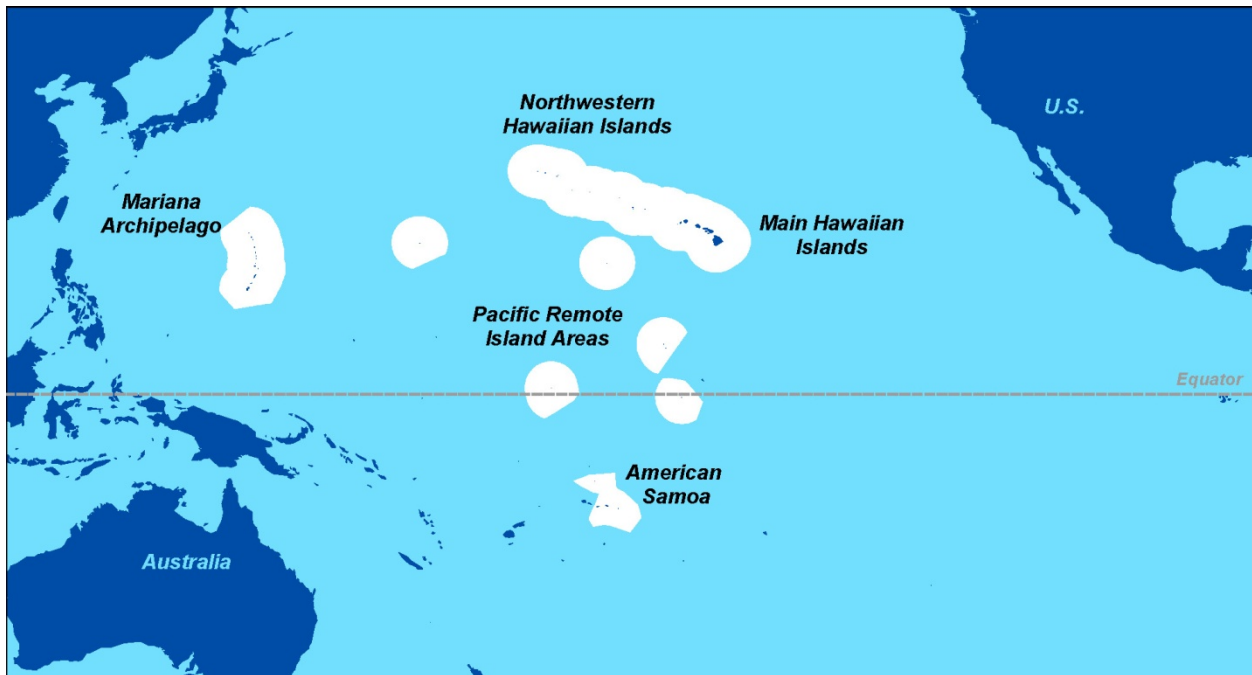
Figure 1.--The Pacific Islands Region, which consists of the Hawaiian and Mariana Archipelagos, American Samoa and the Pacific Remote Island Areas, including seven islands scattered across the tropical Pacific.

High-resolution bathymetric data are essential for characterizing benthic habitats. These data can be acquired using shipboard sonars and satellite or aerial remote sensing techniques. Extensive multibeam sonar data collection has occurred in the U.S. Pacific Islands Region. In the depth range from 0 to 150 m, 48% of the seafloor within the region and 84% of the area outside of the Northwestern Hawaiian Islands has been mapped; however, significant gaps still exist around U.S.-affiliated Pacific islands between 0 and 30 m depths (Miller et al., 2011). This is primarily because multibeam surveys conducted using small boats are often unable to collect data in depths shallower than ~ 10–15 m as a result of navigation hazards associated with shallow reefs; therefore, most islands in the region are left with a ring-shaped gap in bathymetric coverage between the shoreline and approximately ~ 15–30 m. Having bathymetric data for these shallow depths is critical for managers in the Pacific Islands Region where many coral reefs are present,

and exchange of nutrients, sediments, and pollutants between the land and ocean must pass through this zone. It is also an area where many anthropogenic impacts can occur, such as sedimentation, nutrient enrichment, and ship groundings.

By measuring the difference in travel times of two different wavelengths of light (near-infrared [NIR] and green), airborne LiDAR (Light Detection and Ranging) is a technique that can also be used to collect high-resolution depth information in shallow marine environments (Irish et al., 2000). Bathymetric LiDAR data have been collected around many shorelines in the main Hawaiian Islands (MHI) and a few other more populated islands in the region. These data fill the nearshore gap left by multibeam surveys. Unfortunately, the vast majority of islands and shorelines in the Pacific Islands Region lack such coverage. The benefit of LiDAR is that high-resolution data can be acquired over large areas in a very short time, but there are also difficulties associated with this method. At depths shallower than ~ 1 m it becomes difficult to distinguish between the differences in travel times associated with the water surface and bottom returns, and the calculated depths become increasingly ambiguous (Guenther et al., 2000). More importantly, white water and turbidity from breaking waves often prevent the collection of accurate depth data from bathymetric LiDAR in these areas. Therefore, gaps in bathymetric LiDAR often exist.[1] The aforementioned limitations aside, LiDAR still offers the most accurate method to acquire bathymetry over large areas and in water too shallow for multibeam surveys. However, due to the mobilization of equipment and aircraft to conduct surveys at scattered and often remote locations in the Pacific Islands Region, the acquisition of bathymetric LiDAR data is prohibitively expensive for most agencies and stakeholders (Miller et al., 2011).

Since the late 1970s it has been recognized that, as an alternative to the discussed active remote sensing tools (sonar and LiDAR), shallow-water depths can also be estimated using multi-band satellite imagery and passive remote sensing techniques (Lyzenga, 1981; Clark et al., 1987; Philpot, 1989). These methods are effective for mapping shallow-water ecosystems including coral reefs, but they do not provide the same continuity and accuracy as active remote sensing tools (Costa et al., 2009). In recent years, the initially proposed methods have been modified and new methods have been developed (e.g., Maritorena et al., 1994; Stumpf et al., 2003; Mishra et al., 2005; Hogrefe et al., 2008; Kanno, 2012).

Hogrefe et al. (2008) derived depths for 12 islands in the Pacific Islands Region using 4-m resolution multispectral satellite imagery (IKONOS); however, the first IKONOS images were acquired in 1999 and satellite technologies have dramatically improved since. In 2009 DigitalGlobe launched the WorldView-2 (WV-2) satellite, which collects 1.84-m resolution images and includes four new color bands (coastal, yellow, red edge, and NIR2) along with the four common bands (Fig. 2). Further, the greater clear-water depth penetration of the newly introduced coastal band (400–450 nm) supports bathymetric studies (DigitalGlobe, 2009). Here we apply existing methods and develop new techniques as needed to derive high-quality shallow-water bathymetry from WV-2 satellite imagery. This work aids in overcoming the challenges associated with estimating depths for waters shallower than ~ 20 m for the remote, scattered, and heterogeneous study areas of the U.S.-affiliated Pacific islands.

---

[1] http://www.nps.edu/academics/centers/remotesensing/abstracts.html
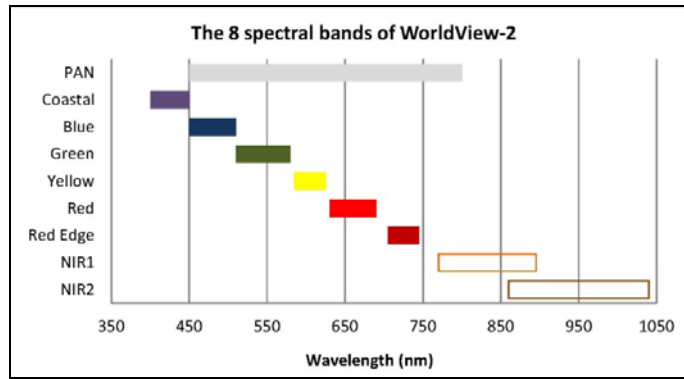
Figure 2.--The EM spectrum range of the eight available spectral bands of the WV-2 satellite image.[2]

DATA AND METHODS

Study area – The goal of this study is to investigate techniques for deriving shallow-water bathymetric data from WV-2 satellite imagery. In the future we intend to apply these methods to our broad study area including all the U.S.-affiliated islands, atolls, reefs, and banks within the Pacific Islands Region that lack bathymetric LiDAR data (see Appendix). For method development and testing we focused on two study areas in the MHI (Fig. 3). Kapoho is the easternmost point on the Island of Hawaiʻi, the largest island in the Hawaiian Archipelago. The initial study area lies north of Kapoho at 19°33'35" N and 154°52'12" W and occupies an area of ~ 11.9 km^2. Niʻihau is the oldest of the MHI and lies at 21°55' N and 160°10' W. It is the second smallest island in the chain (182 km^2) and was inhabited in 2010 by 170 people (State of Hawaiʻi, 2011).
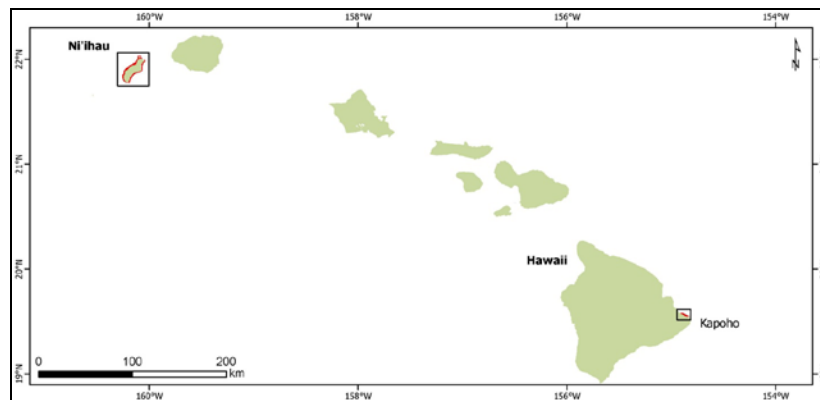
Figure 3.--Initial study areas including Niʻihau Island and a small area north of Kapoho on the Island of Hawaiʻi.

_____

[2] Figure modified after http://worldview2.digitalglobe.com/about/.

Background – Depth derivation using passive remote-sensing methods is based on characteristics of the electromagnetic (EM) spectrum. Visible light, with wavelengths ranging from 380 to 750 nm, is part of the EM spectrum and is transmitted with little attenuation through the atmosphere; however, visible light is attenuated in water with increasing depth. The amount of attenuation is related to the wavelengths of visible light; shorter wavelengths (i.e., coastal and blue) are less attenuated in water than longer wavelengths (i.e., green, yellow, and red). This variable attenuation of the different wavelengths of visible light enables us to correlate seafloor depth and the radiance values of multispectral satellite images.

We previously noted that several early studies developed methods for deriving depths from satellite imagery using properties of the EM spectrum. In this work, we will focus on those of Lyzenga (1978; 1979; 1981; 1985; 2006) and Stumpf et al. (2003), which are the most successful and commonly used methods. Lyzenga (1978; 1981) assumed that a linear relationship exists between depth and the spectral radiance values of a visible band reflected by the seafloor. The Lyzenga method involves extracting spectral radiance values from satellite images for positions with known depths (ground truth points) and using linear regressions to derive a relationship between the radiance and ground truth information. The mathematical relationship is then used to calculate depths for coastal waters across the entire satellite image.

Many studies have successfully derived depths using Lyzenga's method (Hochberg et al., 2007; Hogrefe et al., 2008; Liu et al., 2010; Deidda and Sanna, 2012; Kanno and Tanaka, 2012). This method is popular and has been widely used because it assumes that depth is independent of difficult-to-estimate optical properties, such as bottom type, atmospheric conditions, water quality, and the positions of the sun and satellite. Additionally, Philpot (1989) indicated that including these properties increases the complexity of the model and reduces the reliability of the results; therefore simpler, reproducible methods are preferred.

Clark et al. (1987) and Lyzenga et al. (2006) proposed a multi-band method which helps reduce errors introduced by variations in seafloor bottom type. A multiple linear regression is applied using spectral values from multiple bands. Such an extension of the original method is appropriate when working with 8-band multispectral images; however, to successfully apply Lyzenga's and Clark's methods (hereafter referred to as Lyzenga method), sufficient ground truth points over homogenous seafloor are required. These are often difficult to obtain in remote island areas across the Pacific.

Alternatively, Stumpf et al. (2003) introduced a method requiring only a few ground truth points that achieved good results over heterogeneous bottom types. They used attenuation rates from two spectral bands to develop a reflectance ratio model. The ratio between the blue and green band was used since, with increasing depth, reflected spectral radiance decreases faster in high-absorption bands (green) compared with low-absorption bands (blue); therefore, variations in the band ratio correspond to changes in depth.

Here, both methods (Lyzenga and Stumpf) were first tested in the study area north of Kapoho, where bathymetric LiDAR data are available for depth calculations and error analysis. After successfully deriving depths for North Kapoho, we focused on Niʻihau Island, where the lack of

high quality ground truth points is similar to what is anticipated for many remote and lightly or uninhabited islands throughout the region.

Data

Satellite Images – The WV-2 data used in this study were collected on January 2, 2010, with an average cloud cover of 5% for Niʻihau Island. The imagery for Kapoho was collected December 11, 2010, with an average cloud cover of < 1%. The quality of each image varies and depends on the environmental conditions on the day of acquisition. Factors like cloud cover, shallow-water turbidity, high surf, whitewash, and sunlight reflectance on wave slopes severely impact derived results; therefore, these noisy areas are manually masked out and sea surface corrections are performed before deriving depth.

Ground Truth Data – Bathymetric ground truth data are required for depth calculations and subsequent error analysis. Figure 4 shows the extent of LiDAR bathymetry coverage for the area north of Kapoho, Hawaiʻi.
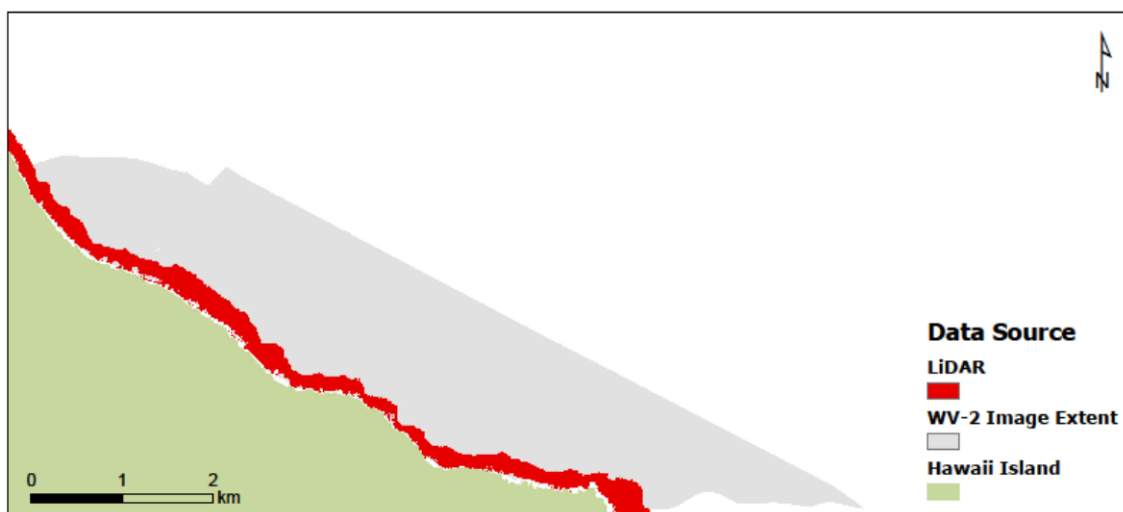
Figure 4.--The extent of LiDAR coverage north of Kapoho on the Island of Hawaiʻi.

Insufficient multi-beam bathymetry coverage and the absence of bathymetric LiDAR data around Niʻihau require the use of other, and in some cases less reliable, data sources to derive depth.

Four different types of ground truth data were compiled (Fig. 5).

1. Multi-beam bathymetry – The most accurate and highest resolution depth data available are from a 5-m resolution multi-beam grid.[3] Unfortunately, within the study area these

---

[3] Available from http://www.soest.hawaii.edu/pibhmc.

data are limited to 16–20 m depths, lacking much of the depth range of interest (0–20 m) and geographic extent necessary for them to be useful for depth calculations.

2. Rapid Ecological Assessment (REA) – Depth and habitat data were collected by CRED scientists during dive surveys. Each depth data point is measured using a dive computer held at the seafloor and provides an accurate seafloor measurement with good horizontal positional accuracy; however, the limited number of data points and the recording of depth values as integers limits their usefulness for model building.

3. Towed Diver – Depth and habitat data were collected by CRED scientists during towed-diver surveys (Kenyon, 2004). Each depth point is measured and recorded by an SBE 39 conductivity, temperature, depth (CTD) instrument (Sea-Bird Electronics Inc., Bellevue WA) with a pressure sensor. Depths are measured approximately 1 m above the seafloor. Although less accurate than multibeam or REA data (due to less horizontal positional accuracy and variable altitude of diver above seafloor), the towed-diver data are well distributed across the study area and are therefore useful for this analysis.

4. Electronic Navigational Chart (ENC) – Nautical chart data are collected and developed by NOAA to insure safe navigation in U.S. waters. Most of the ENCs are based on NOAA nautical paper charts with an average horizontal accuracy of ±10 m according to Differential Global Positioning System[4]; however, the underlying data sources for nautical charts have been collected over a long period of time by various sources resulting in a much higher error due to inconsistent depth information within a particular location. Therefore, the suitability of these datasets for depth derivation models is questionable.

---

[4] http://www.nauticalcharts.noaa.gov/nsd
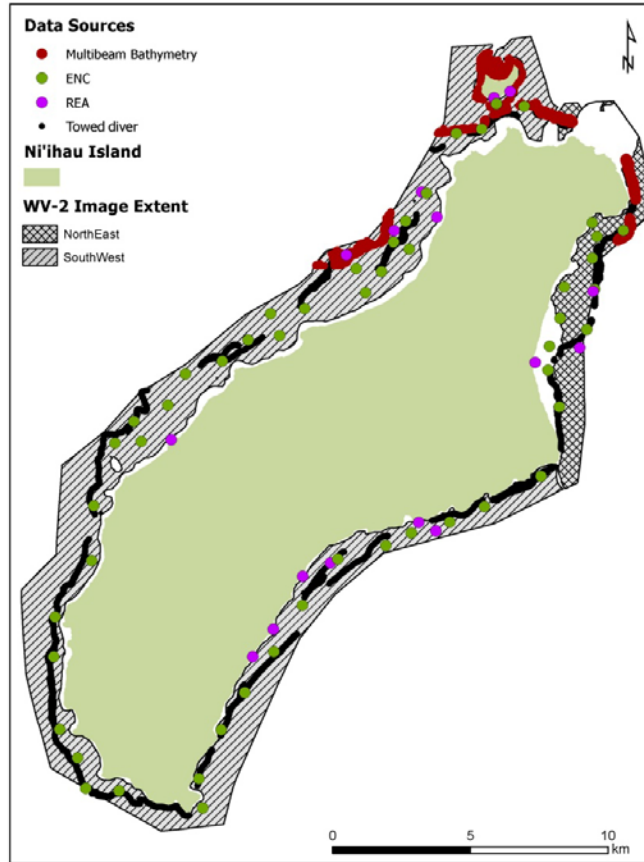
Figure 5.--Shown is the distribution and availability of four different ground truth data types around Ni'ihau Island: multibeam bathymetry, REA, towed-diver and ENC. The WV-2 image extension is shown in different grey symbols.

Methods

Image Preprocessing – Three image preprocessing steps were performed before deriving depths.

Data Conversion

The raw WV-2 multi-band satellite data are provided as digital numbers (DNs). These DN values were converted to top-of-atmosphere (TOA) radiance using the calibration factor and effective bandwidth for each band supplied by DigitalGlobe in the image metadata file (.imd) and the following equation:

$$R_i = \frac{K_i \times DN_i}{\Delta\lambda_i} \qquad (1)$$

7

where R_i is TOA radiance for band i, K_i is the absolute radiometric calibration, and $\Delta\lambda_i$ is the effective bandwidth for band i.

Masking

It is important to eliminate all nonaquatic objects from the image before deriving depths. By creating an ocean mask, all terrestrial areas and detailed features like clouds, turbidity (caused by freshwater runoff), breaking surf, and boats were removed from the image. The mask was manually created in ArcGIS by drawing polygons around the areas of interest and extracting the spectral radiance values from the image.

Sea Surface Corrections

Passive remote sensing is most effective if images are acquired in conditions with minimal atmospheric disturbances and clear water; however, almost every image is contaminated by reflected light (sun glint) from the ocean surface. Sun glint appears as white stripes along the slope and crest of a wave, but radiance values can still be extracted from these areas (Deidda and Sanna, 2012). A method proposed by Hochberg et al. (2003) and modified by Hedley et al. (2005) allows for the correction of sun glint in visible bands from satellite images (Eq. 2). This technique is based on two assumptions: 1) measured radiance in the NIR portion of the EM spectrum represents sun glint, and 2) the magnitude of sun glint in the NIR is linearly related to the amount of sun glint in the visible bands. Therefore, the NIR value will indicate the amount of sun glint in the visible portion of the EM spectrum (Hedley, 2005). Extracting pixel values from a portion of an image over optically deep water and performing a linear regression on the NIR band radiance values (dependent variable) versus the visible band values (independent variable) allows us to extract the measured light reflectance value from each pixel in each band and deglint the entire image using the following equation (Hedley, 2005):

$$R'_i = R_i - b_i(R_{NIR} - min_{NIR}) \qquad (2)$$

where R'_i is the glint and atmosphere corrected image for band i, R_i is the uncorrected image, b_i is the slope resulting from the regression of band i, R_{NIR} is the NIR radiance, and min_{NIR} is the minimum NIR value.

Depth Derivation Processes

Lyzenga's multiple linear regression analysis—A multiple linear regression analysis was applied using spectral radiance values for coastal, blue, green, and yellow bands as the independent variables and depth as the dependent variable. A point shapefile was generated in ArcMap to obtain coincident deglinted spectral radiance and depth values using the ArcGIS sample tool, which creates a table for a set of input rasters (depth data and deglinted satellite image) at specific locations (point shapefile). The number of points per shapefile depends on the availability of ground truth data. A subset of these points was used for the linear regression and the remaining points for error analysis. The y-intercept and slope for each spectral band resulting from the multiple linear regression analysis were used to derive depth using the following equation, which is a multi-band version of the original Lyzenga method (Clark et al., 1987; Lyzenga et al., 2006):

$$D = a + (b_1)(R''_1) + (b_2)(R''_2) + (b_3)(R''_3) + ... + (b_n)(R''_n) \qquad (3)$$

where D is depth, a is the y-intercept, b is the slope, R''_i is $ln\ (R'_i - min(R'_i))$, and $i = 1,2,3,...,n$ corresponds to the number of bands.

Note that in the original Lyzenga method shown in Equation 3 the spectral radiance values are linearized by subtracting the minimum spectral radiance value of each band from all the band values and taking the natural log of the resulting spectral radiances.

Stumpf's ratio method--The ratio method is expressed by the following equation:

$$D = m_1 \frac{\ln(nR''_1)}{\ln(nR''_2)} m_0 \qquad (4)$$

where D is depth, m_1 is a tunable constant to scale the ratio to depth, n is a constant to keep the ratio positive, R''_1 is the band 1 radiance of light reflected off the water surface, R''_2 is the band 2 radiance of light reflected off the water surface, and m_0 is a correction for zero depth.

Stumpf et al. (2003) used blue and green bands to extract spectral values for the ratio method. Here we used the coastal and yellow bands to take advantage of the deeper penetration of the coastal band, which is less absorbed by water than the other bands. The combination of the yellow and blue band resulted in a higher correlation with depth than for the blue and green bands (Alsubaie, 2012). To implement the ratio method we computed relative bathymetry from a subset of the deglinted image using the following equation:

$$relativebathymetry = \frac{\ln(nR''_1)}{\ln(nR''_2)} \qquad (5)$$

where R''_1 and R''_2 are coastal and yellow bands, respectively, of the deglinted image, and $n = 1000$.

The relative bathymetry was then scaled to absolute bathymetry by generating a new point shapefile. For the depth model a few (~10) ground truth data points are needed, but it is still important to reserve a subset for the error analysis. Using the ArcGIS sample tool relative depth values were extracted using the designated model building data points.

Next, m_i and m_0 were estimated by applying a linear regression analysis in which bathymetry was the dependent variable and relative bathymetry is the independent variable. Absolute depth was then calculated using the following equation:

$$D = m_1(relativebathymetry) - m_0 \qquad (6)$$

where D is depth, m_1 is the slope, and m_0 is the y-intercept.

RESULTS

Initially we tested both the Lyzenga and Stumpf methods on a small area around Kapoho, Hawai'i. We performed this test because extensive ground truth LiDAR data exist for the region. The Kapoho WV-2 image contains significant amounts of glint but it was still possible to derive depths after applying the sea surface corrections described above.

Lyzenga's Method

Figure 6 shows depth derived from applying the Lyzenga method (Eq. 3) to the Kapoho satellite image vs. LiDAR depths. Many of the derived depth values are zero whereas the corresponding LiDAR depths are nonzero suggesting the method overcorrects the spectral radiance values resulting in a weak relationship between derived and LiDAR depths ($R^2 = 0.19$). This problem is specific to the shorter wavelengths (i.e., blue and coastal bands) and may be caused by taking the natural log of the spectral radiance values prior to performing the multiple linear regressions.
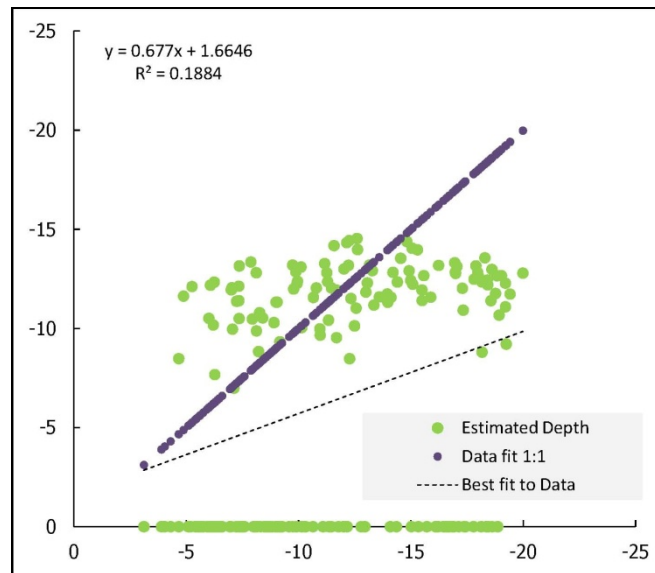
Figure 6.—Ground truth LiDAR bathymetry vs. estimated depths. Results of the Lyzenga method are shown as green diamonds. The purple squares are for reference and indicate how perfect recovery of the LiDAR depths would plot.

For that reason, we adopted a modified approach by eliminating the linearization step and performing the multiple linear regressions on the deglinted spectral radiance values from Equation 2. This resulted in a much stronger correlation between the ground truth LiDAR data and the deglinted spectral radiance values (R = 0.78; Table 1, *right*) compared with the linearized

spectral radiance values and LiDAR data (R = 0.58; *left*). This suggests the relationship between these data is already linear and that taking the natural log of spectral radiance values $(R'_i - min(R'_i))$ is unnecessary.

Table 1.--Comparison of two different multi-linear regression using LiDAR vs. logarithmic deglinted spectral radiance values (left) resulting in a weak relationship ($R^2 = 0.33$) and LiDAR versus deglinted radiance values (right) resulting in a stronger relationship between the data ($R^2 = 0.60$).

	Linearized Spectral Radiance	Deglinted Spectral Radiance
Multiple R	0.58	0.78
R Square	0.33	0.60
Adjusted R Square	0.31	0.59
Standard Error	3.09	2.39
Observations	122	122

Figure 7 shows a plot of the depths derived using nonlinearized spectral radiance values vs. the ground truth LiDAR depths. The relationship between bathymetric LiDAR and derived bathymetry is significant ($R^2 = 0.83$; *left*). The absolute mean difference between estimated depth and LiDAR depth is 1.74 m. Furthermore, the 95% confidence interval limits of the derived depth values are 2.83 m and -5.16 m. The plot shows that accuracy decreases with increasing depth (*right*). If depth differences are limited to LiDAR depths of 0 to 15 m, the absolute mean difference between estimated depth and LiDAR depth is 0.98 m with 95% confidence interval limits of 2.59 and - 0.62.
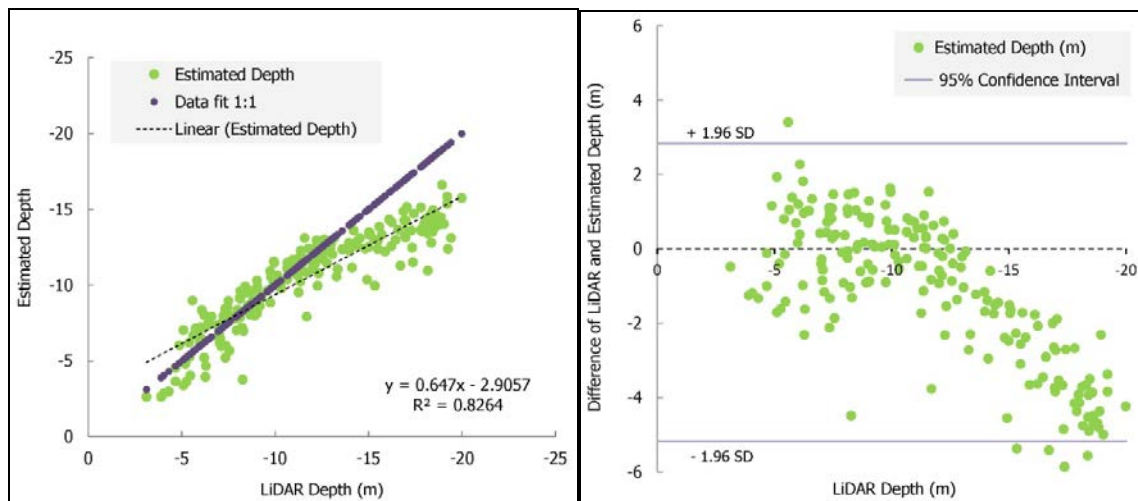

Figure 7.--LiDAR vs. estimated depth with $R^2 = 0.83$ indicating a strong correlation between the data (left). Bland-Altman plot showing the differences between LiDAR and estimated depths vs. LiDAR depths, and the 95% confidence interval limits of + 2.83 m and - 5.16 m (right).

The map below (Fig. 8) shows gridded estimated bathymetry for north Kapoho, using nonlinearized spectral radiance values for the multiple linear regression analysis. Depth calculations reach ~ 39 m whereas the extent of the satellite image covers areas with depths > 600 m. The seafloor around the MHI is known to have steep slopes and significant depth drop-offs within 1 km offshore. Further, Figure 9 highlights also that the accuracy of derived depth decreases with increasing depth. In this region seafloor depths < ~ 20 m are accurate within ~ 5 m and errors increase with depths > ~ 20 m. These results suggest that derived depth values > 20 m should be disregarded in this region.
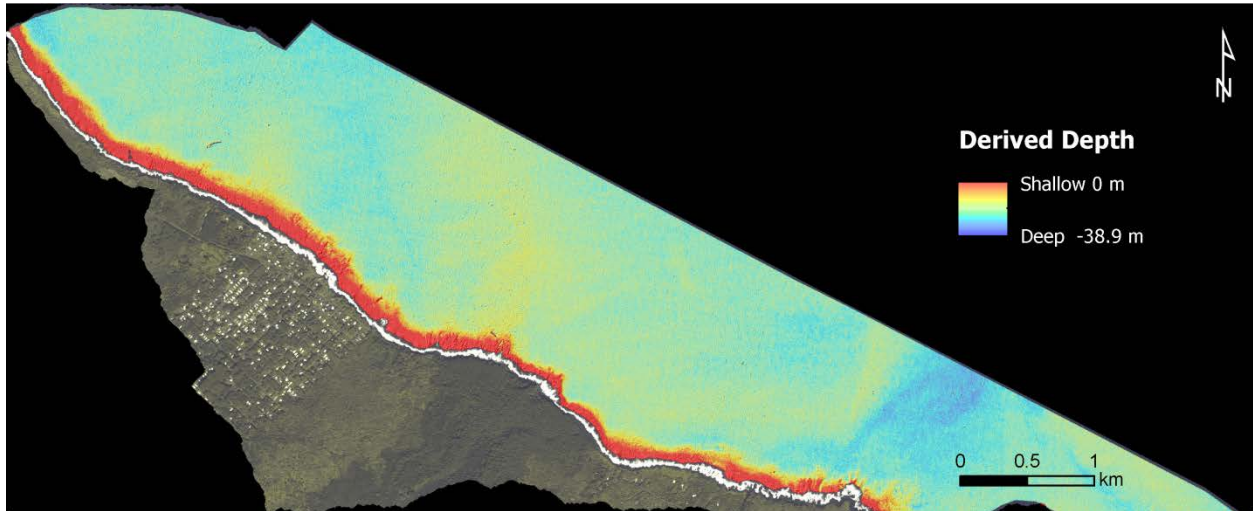
Figure 8.--Map of gridded estimated bathymetry generated by performing a multiple linear regression analysis on the nonlinearized spectral radiance values.

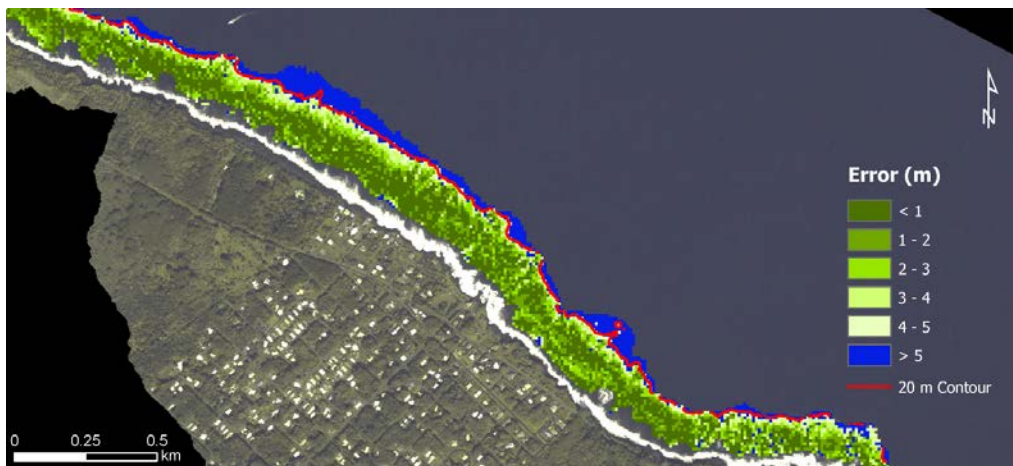Figure 9.--Map showing the absolute difference between bathymetric LiDAR and estimated depth by performing a multiple linear regression analysis on the nonlinearized spectral radiance values. Green shows locations where the difference is < 5 m. Blue shows locations where the difference is > 5 m, which approximately corresponds to the 20-m depth contour shown in red.

Stumpf and Holderied's Ratio Method

Results for the ratio method are shown in Figure 10. A poor relationship between LiDAR and derived depth is reflected by the R^2 value of 0.22 (Fig. 10, *left*). The mean absolute difference of the two data sets is 3.17 m. Furthermore, the 95% confidence interval limits of the derived depth values are - 8.52 m and + 6.3 m (*right)* suggesting the method results in less accurate derived bathymetry compared to Lyzenga's method.
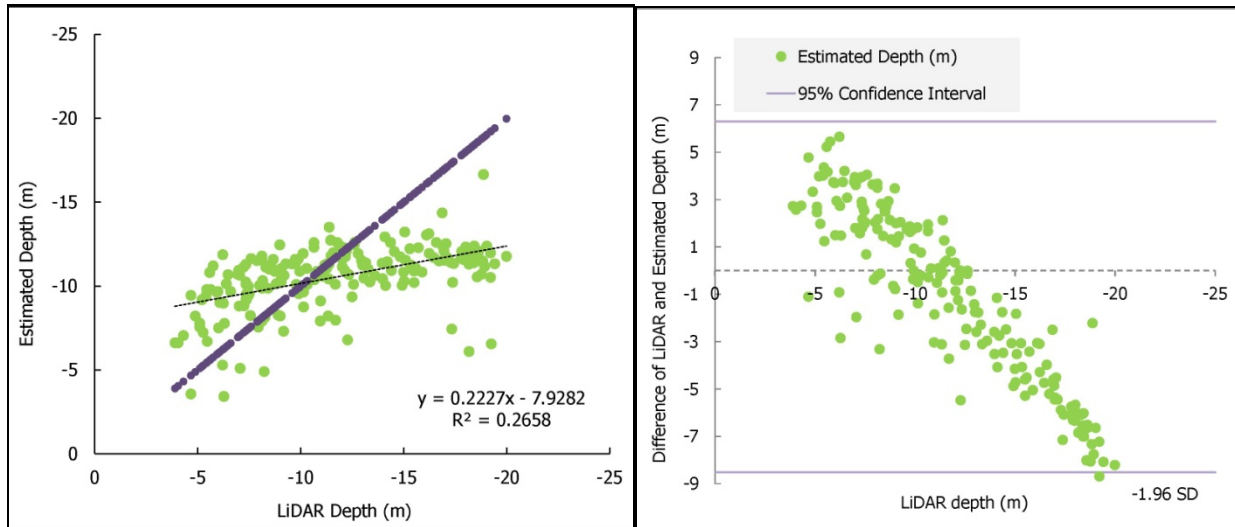
Figure 10.--LiDAR vs. estimated depth using coastal and yellow spectral radiance values in the ratio method. R^2 = 0.22 shows a weak correlation between the two data sets (left). The absolute mean difference is 3.2 m and the 95% confidence interval ranges from 6.3 m and - 8.5 m (right).
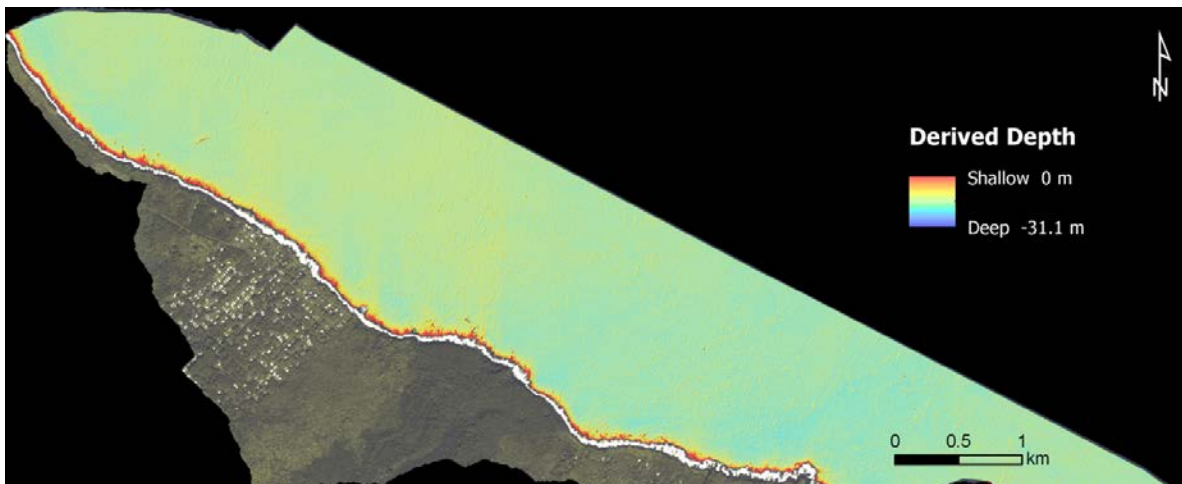
Figure 11 shows the results of the ratio method in map view. The maximum calculated depth is ~ 31 m and only a few of the morphological features are detected in the very shallow areas.

A direct comparison of derived depths from the Lyzenga and Stumpf methods to bathymetric LiDAR is shown in Figure 12. The red boxes highlight linear morphological features that extend from the shoreline out to ~ 20 m that can be compared across the different data sets. The Lyzenga method matches bathymetric LiDAR and does the best job of recovering the detailed seafloor morphology.
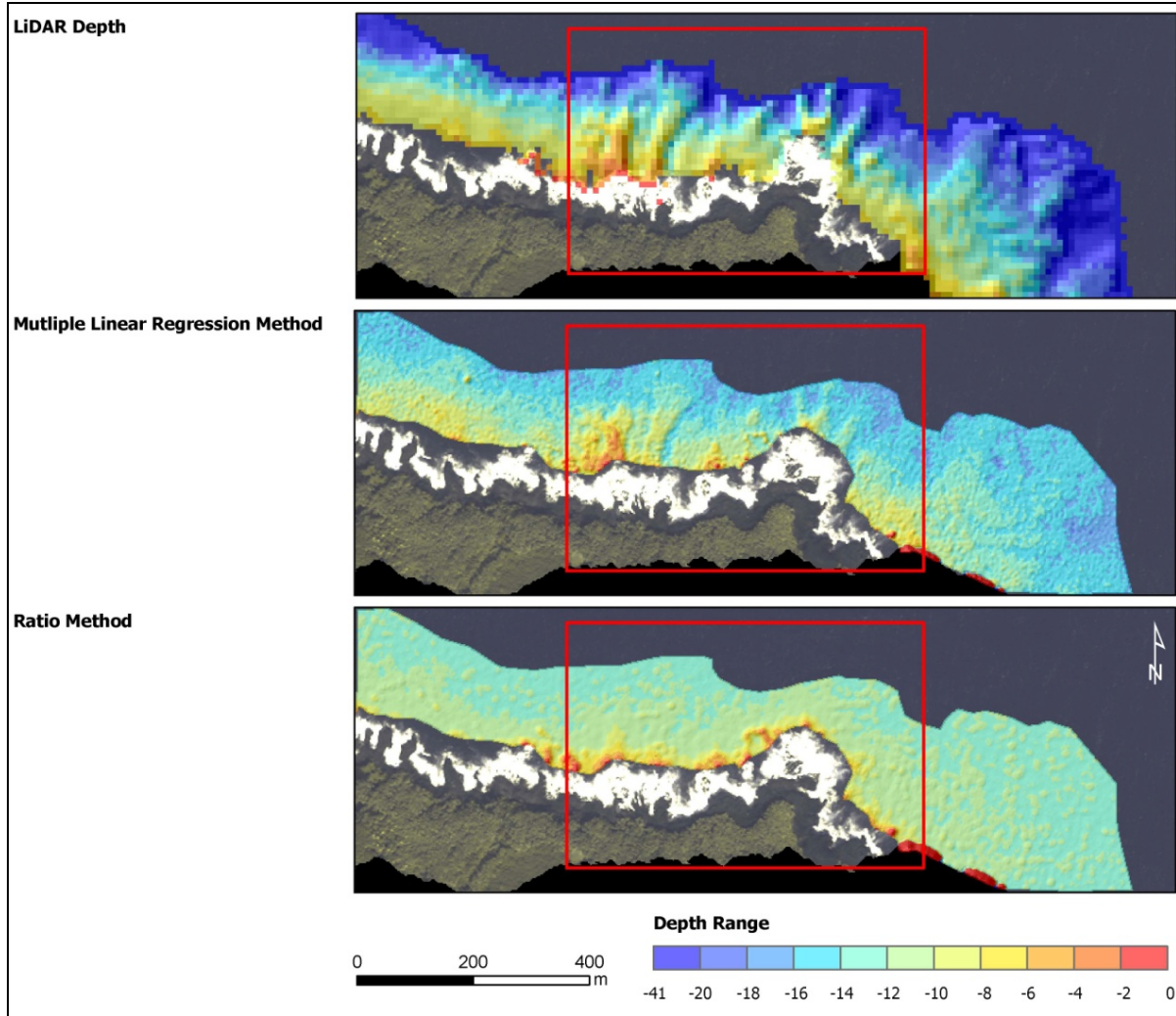
Figure 12.--Map showing a small section of LiDAR bathymetry for Kapoho, Hawai'i in 10×10 m resolution compared to estimated bathymetry for multiple linear regression method and ratio method in 2×2 m resolution.

Ni'ihau Application

Based on our results for Kapoho we decided to apply the Lyzenga method to our study area around Ni'ihau and to use a nonlinearized data set. Two WV-2 image mosaics were available for Ni'ihau; one covered the southwest portion of the island and the other covered a small area

located in the northeast (Fig. 5). We performed two independent depth derivations to generate bathymetry for the entire Island.

As mentioned earlier (Section: Data and Methods), the amount of available ground truth data for Niʻihau differs tremendously from the Kapoho, Hawaiʻi area. Since LiDAR bathymetry is completely lacking there, we used a combination of ENC, REA, and multibeam bathymetry data to perform our analysis (Fig. 5). Initially, towed-diver data were excluded from the analysis because of its limitation in horizontal accuracy. The process entailed compiling ground truth data for the southwest portion of the island; extracting coastal, blue, green, and yellow spectral band values for selected depth points; performing the multiple linear regression analysis; and computing derived depths for southwest Niʻihau.

Initial results showed a weak relationship between derived depth and ground truth data ($R^2 = 0.42$). To test whether this was caused by incorporating different ground truth data types (each with their own inherent errors) in the analysis, the model was rerun using only towed-diver data. These data cover a larger depth range (5–20 m) and a sufficient number of data points exist to apply the model and to perform an independent error analysis. Prior to computing estimated depths, we first added 1 m to each towed-diver data point to account for the survey height above the seafloor. Figure 13 shows the results of the analysis, which are significantly better than the initial results with $R^2 = 0.71$ (*left*), and the 95% confidence interval limits are + 3.1 m and - 3.5 m. Furthermore, the mean absolute difference between derived depths and tow depths is 1.2 m with a maximum difference of 6.7 m between the data sets (*right*).
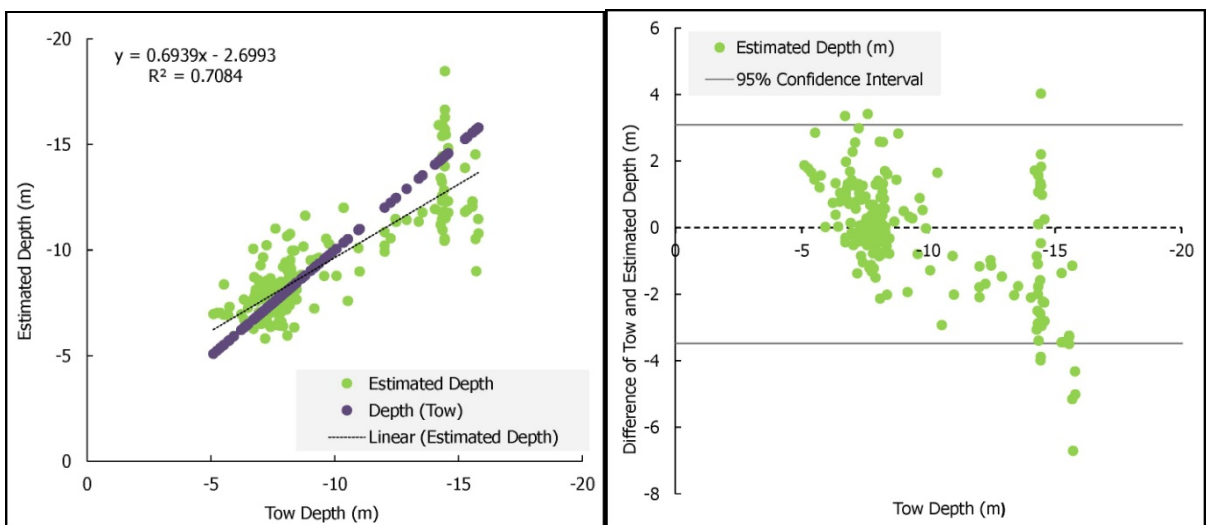
Figure 13.--Tow vs. estimated depth with $R^2 = 0.71$ indicating a strong correlation between the data (left). The difference between estimated depth and tow depth are shown (right). The 95% confidence interval is at 3.1 m and -3.5 m. The high density of tow depth data points at ~-15 m is a reflection of the target depth for towed-diver surveys.

The process was repeated for the smaller northeast Niʻihau area again using only towed-diver data. Results are shown in Figure 14. The process was less successful than for southwest Niʻihau

resulting in an R^2 value of 0.59 (*left*). The 95% confidence interval limits are +5.4 m and -5.3 m and the mean absolute difference is 2.1 m (*right*).
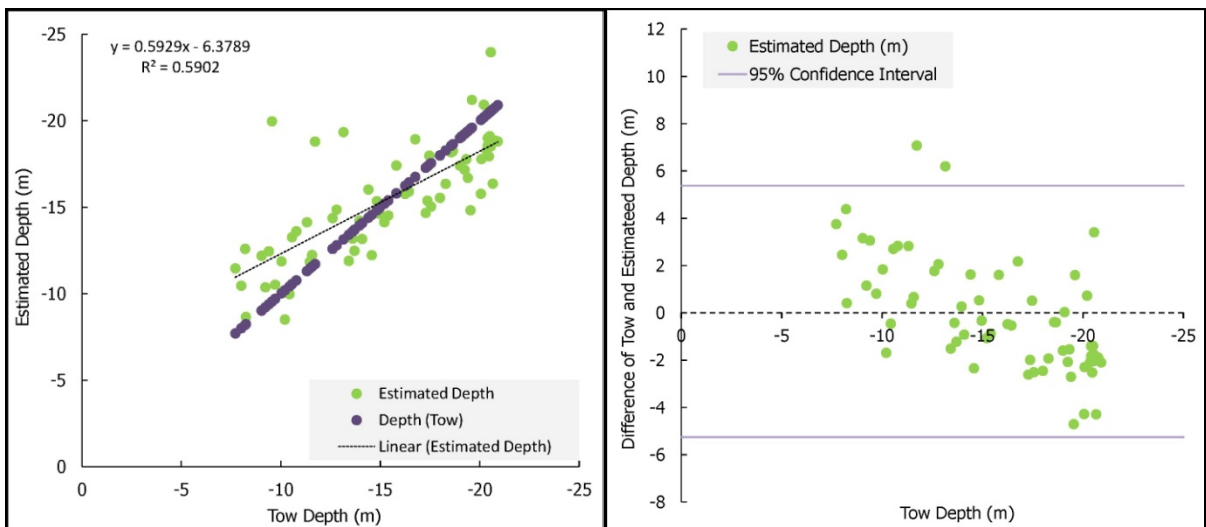
Figure 14.--Tow vs. estimated depth with $R^2 = 0.59$ indicating a good correlation between the data (left). Bland-Altman plot showing the differences between LiDAR and estimated depths vs. LiDAR depths, and the 95% confidence interval limits of + 5.4 m and - 5.3 m (right).

For the final step we mosaicked both derived depth data grids into one grid for Niʻihau (Fig. 15). Existing data gaps are a result of whitewash along the shoreline, cloud coverage, breaking waves, WV-2 image data gaps, high turbidity, and heavily glinted areas.

16
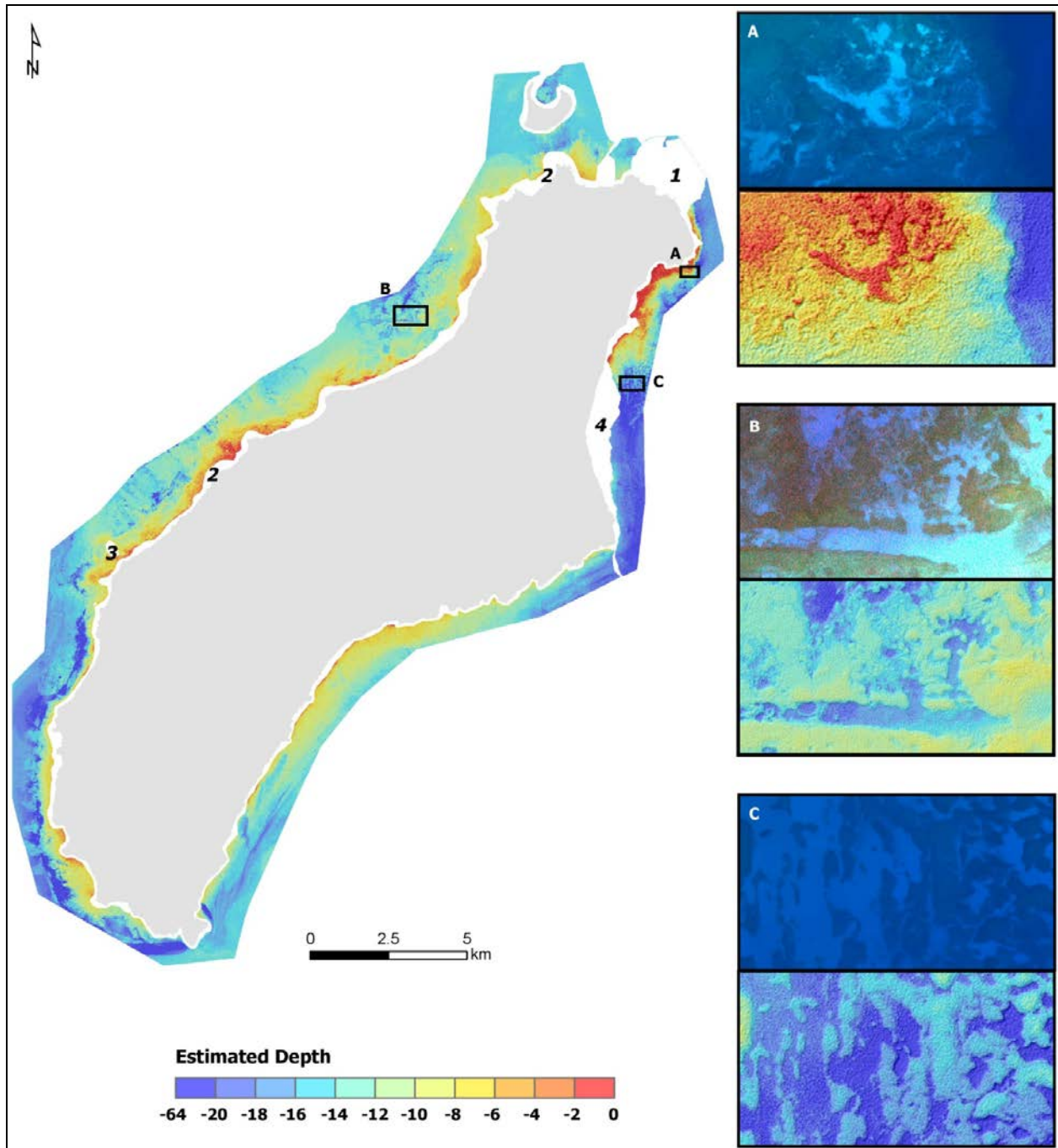
Figure 15.--Map of the estimated bathymetry derived using the multiple linear regression method including deglinted spectral radiance values and towed-diver data. The model is able to recover detailed seafloor features like channels (B) and coral reefs (C). There is a small area on the northeast side of the island where highly reflective areas appear too shallow (A). Data gaps are related to cloud cover (1), whitewash (2), breaking waves around rocks (3), and WV-2 data gaps (4).

DISCUSSION AND CONCLUSION

The main objective of this study was to investigate two of the most commonly used techniques (Lyzenga and Stumpf) for shallow-water depth derivation using WV-2 satellite imagery to help fill shallow-water bathymetry gaps. Furthermore, of the two methods we wanted to identify, the most feasible one in terms of quality and usability that can be applied to our broad study area across the remote Pacific Islands Region.

Our results show that the Lyzenga multiple regression method was successful in deriving depths for both of our study areas (Kapoho, Hawaiʻi, and Niʻihau) when using only the deglinted spectral radiance values instead of the linearized and deglinted spectral radiance values. Taking the natural log of spectral radiance values (Eq. 3) gave erroneous results. This problem occurs because the minimum radiance value for each spectral band over optically deep water is difficult to obtain (Doxani et al., 2012). Therefore, deglinted spectral radiance values are sometimes lower than the "minimum" deglinted spectral radiance values resulting in negative radiances when Equation 3 is applied, and undefined values when the natural log is taken.

Doxani et al. (2012) discovered that the presence of sea grass affects the linear relationship between ground truth depth and spectral radiance values negatively, causing the multiple linear regression analysis to fail. The MHI lack large sea grass aggregations; this may explain the observed linear relationship between depth and spectral radiance values in our study areas and eliminate the need to linearize the data using the natural log portion of Lyzenga's method.

We successfully derived depth using LiDAR (Kapoho) and towed-diver (Niʻihau) data, although the accuracy of our derived product is highly dependent on the quality of the available ground truth data. There are some limitations to the accuracy of towed-diver data; namely, a degree of uncertainty about the horizontal positional accuracy of the data as well as some variability in the elevation of the diver above the seafloor. Despite these errors, the multiple linear regression analysis recovered detailed seafloor features like spur and groove (Fig. 12), channels, and reef-like structures (Fig. 15). Unfortunately, we also experienced problems deriving depth in the shallow areas with high albedo over sandy bottom, where the seafloor appears to be too shallow (Fig. 15). This problem is common amongst many studies. Mishra et al. (2005) explains this kind of failure in depth estimations by heterogeneous bottom substrates with significant differences in albedos; dark bottom absorbs more light and will therefore appear deeper than its surrounding bright bottom with less absorption capacity.

The accuracy of estimated depth decreases with increasing depth showing mean absolute differences between data sets of approximately 2 m in depths < 20 m and > 5 m in depths > 20 m. This suggests we should use 20 m as a cutoff when integrating the derived depths with deeper data such as multibeam sonar. This is the case for the study sites presented here. We may be able to improve the accuracy of the derived product at greater depths for other study sites if the satellite imagery is of sufficient quality; however, Hochberg et al. (2007) suggests the same cut-off depth for his study site on Oahu, Hawaiʻi, using Lyzenga's multiple linear regression analysis. The estimated depth results presented here capture the general topography of the

18

seafloor and are reasonably accurate, with results comparable to or better than those of other studies (e.g., Hogrefe et al., 2008; Su et al., 2008; Mishra et al., 2005).

The application of the Stumpf et al. depth derivation model was not effective for Kapoho and therefore was not tested on Niʻihau. More study sites are needed to determine if a single method can be applied everywhere, or if methods must be modified on a site-by-site basis depending on the quality of the ground truth data and the satellite imagery available.

Despite the aforementioned limitations in data accuracy, the use of satellite-derived depths is an effective method for mapping the shallow-water areas (0–20 m) where coral reef environments are found. Especially in remote areas where it is too untimely and costly to acquire multibeam and LiDAR bathymetry, satellite-derived depths can serve as valuable information for decision makers, including managers and stakeholders within the Pacific Islands Region.

ACKNOWLEDGMENTS

REFERENCES

Alsubaie, N.; Elhabiby, M.; El-Sheimy, N.
  2012. The Potential of Using Multi-Spectral Satellite Imagery for Shallow Water Bed
  Mapping. The Seventh National GIS Symposium in Saudi Arabia. 1–11.

Clark, K. R.; Fay, T. H.; Walker, C. L.
  1987. Bathymetry calculations with Landsat 4 TM imagery under a generalized ration
  assumption. Optical Society of America. Reprinted 1987 by Applied Optics.
  26(19):4036–4038.

Costa, B. M.; Battista, T. A.; Pittman, S. J.
  2009. Comparative evaluation of airborne LiDAR and ship-based multibeam SoNAR
  bathymetry and intensity for mapping coral reef ecosystems. Remote Sensing of
  Environment. 113:1082–1100.

Deidda, M.; Sanna, G.
  2012. Pre-processing of high resolution satellite images for sea bottom. Italian Journal of
  Remote Sensing. 44(1):83–95.

DigitalGlobe.
  2009. The Benefits of the 8 Spectral Bands of WorldView-2. White Paper. 1–10.

Doxani, G.; Papadopoulou, M.; Lafazani, P.; Pikridas, C.; Tsakiri-Strati, M.
  2012. Shallow-water Bathymetry Over Variable Bottom Types Using Multispectral
  WordView-2 Image. International Archives of the Photogrammetry, Remote Sensing and
  Spatial Information Science. XXII ISPRS Congress, Melbourne, Australia.
  XXXIX(B8):159–164.

Guenther, G. C.; Cunningham, A. G.; LaRocque, P. E.; Reid, J. D.
  2000. MEETING THE ACCURARCY CHALLENGE IN AIRBORNE LIDAR
  BATHYMETRY. Proceedings of EARSeL-SIG-Workshop LIDAR, Dresden, FRG. 1:1–
  27.

Hedley, J. D; Harborne, A. R.; Mumby, P. J.
  2005. Simple and robust removal of sun glint for mapping shallow-water benthos.
  International Journal of Remote Sensing. 26(10):2107–2112.

Hochberg, E. J.; Andrefouet, S.; Tyler, M. R.
  2003. Sea surface correction of high spatial resolution IKONOS images to improve
  bottom mapping in near-shore environments. IEEE Transactions on Geoscience and
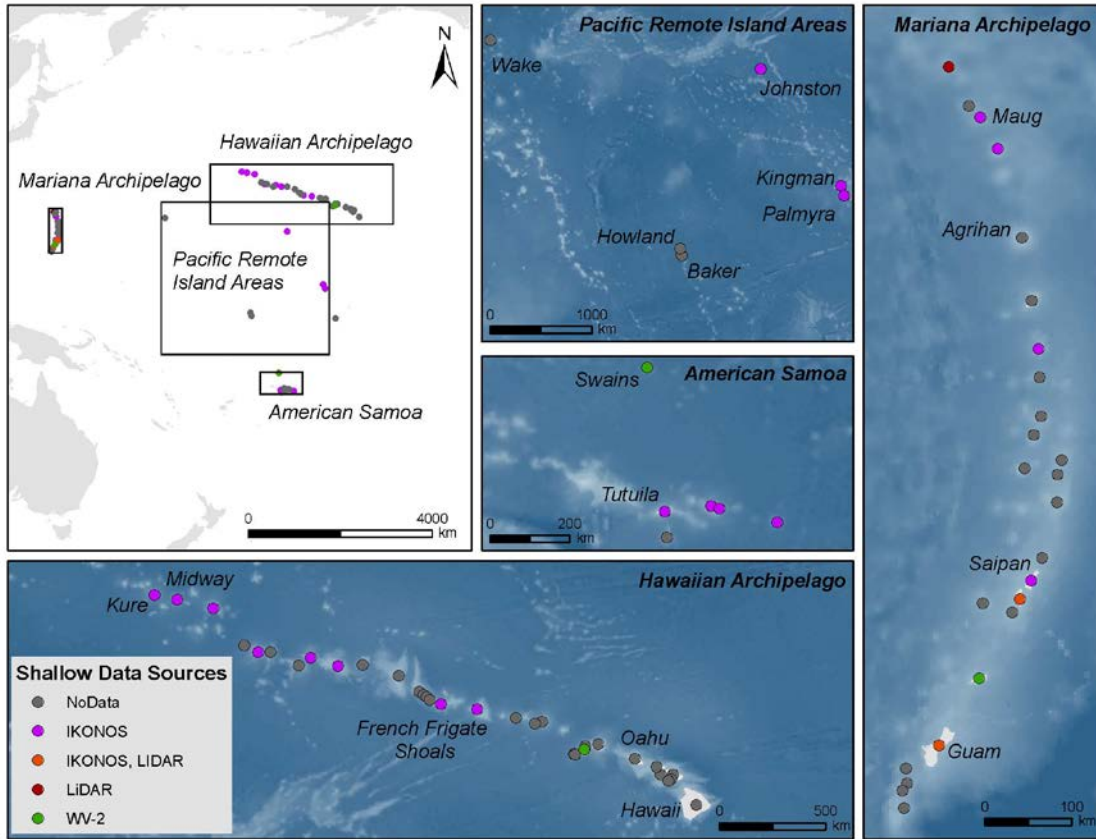 Remote Sensing. 41(7):1724–1729.

Hochberg, E. J.; Vogt, S.; Miller, J. E.; Hogrefe, K. R.
    2007. Remote Sensing of shallow water bathymetry for integration with multibeam SONAR data. Pacific Region Integrated Data Enterprise principle investigators conference, Honolulu, HI. Poster. Online at http://www.soest.hawaii.edu/pibhmc/pibhmc_documentation.htm. [accessed 11 March 2012].

Hogrefe, K. R.
    2009. Derivation of Near-shore Bathymetry from Multispectral Satellite Imagery used in a Coastal Terrain Model for the Topographic Analysis of Human Influence on Coral Reefs. Masters of Science thesis. State University. Oregon, Corvallis.

Hogrefe, K. R.; Wright, D. J.; Hochberg, E. J.
    2008. Derivation and Integration of Shallow-water Bathymetry: Implications for Coastal Terrain Modeling and Subsequent Analyses. Marine Geodesy. 31:299–317.

Irish, J. L.; McClung, J. K.; Lillycrop, W. J.
    2000. Airborne LiDAR bathymetry: the SHOALS system. PIANC Bulletin. 2000(103):43–53.

Kanno, A.; Tanaka, Y.
    2012. Modified Lyzenga's Method for Estimating Generalized Coefficients of Satellite-based Predictor of Shallow water Depth. IEEE Geoscience and Remote Sensing Letters. 9(4):715–719.

Kenyon, J. C.
    2004. Towed-diver Surveys, A Method for Mesoscale Spatial Assessment of Benthic Reef Habitat: A Case Study at Midway Atoll in the Hawaiian Archipelago. Proceedings of the Coastal Zone Asia Pacific Conference. 348–356.

Liu, S.; Zhang, J.; Ma, Y.
    2010. Bathymetric ability of SPOT-5 multi-spectral image in shallow coastal water. Geoinformatics, 2010 18th International Conference. 1–5.

Lyzenga, D. R.
    1978. Passive remote sensing techniques for mapping water depth and bottom features. Applied Optics. 17(3):379–383.

Lyzenga, D. R.
    1979. Shallow-water reflectance modeling with applications to remote sensing of ocean floor. Proceeding of 13th International Symposium on Remote Sensing of Environment. 583–602.

Lyzenga, D. R.
    1981. Remote sensing of bottom reflectance and water attenuation parameters in shallow water using aircraft and LANDSAT data. International Journal of Remote Sensing. 2(1):71–82.

Lyzenga, D. R.
    1985. Shallow-water bathymetry using combined LiDAR and passive multispectral scanner data. International Journal of Remote Sensing. 6(1):115–125.

Lyzenga, D. R.; Malinas, N. R.; Tanis, F. J.
    2006. Multispectral bathymetry using a simple physically based algorithm. IEEE Transactions on Geoscience and Remote Sensing. 44(8):2251–2259.

Maritorena, S.
    1994. Diffuse reflectance of oceanic shallow waters: Influence of water depth and bottom albedo. American Society of Limnology and Oceanography. 39(7):1689–1703.

Miller, J.; Battista, T.; Pritchett, A.; Rohmann, S.; Rooney, J.
    2011. Coral Reef Conservation Program Mapping Achievements and Unmet Needs. NOAA Coral Reef Conservation Program.

Mishra, D. R.; Narumalani, S.; Rundquist, D.; Lawson, M.
    2005. High-resolution Ocean Color Remote Sensing of Benthic Habitats: A Case Study at the Roatan Island, Honduras. IEEE Transactions on Geoscience and Remote Sensing. 43(7):1592–1604.

Philpot, W. D.
    1989. Bathymetric mapping with passive multispectral imagery. Applied Optics. 28(8):1569–1578.

State of Hawai'i.
    2011. Island Population and Housing Units, State of Hawai'i: 2010. Dept. of Business, Economics and Tourism. Research and Economic Analysis Division. Statistics and Data Support Branch. Hawai'i State Data Center. 3.

Stumpf, R. P.; Holderied, K.; Sinclair, M.
    2003. Determination of water depth with high-resolution satellite imagery over variable bottom types. American Society of Limnology and Oceanography. 48(2):547–556.

Su, H.; Liu, H.; Heyman, W. D.
    2008. Automated Derivation of Bathymetric Information from Mult-Spectral Satellite Imagery Using a Non-Linear Inversion Model. Marine Geodesy. 31: 281–298.

List of U.S. Pacific Island Regions showing availability of shallow-water bathymetry derived from IKONOS, WV-2 multispectral satellite imagery, and LiDAR data.

Shallow-water bathymetry in the U.S. Pacific Island Region derived from LiDAR, IKONOS, and WV-2 data.

Marianas	Derived Bathymetry
Agrihan	
Aguijan	
Alamagan	IKONOS
Anatahan	
Asuncion	IKONOS
Farallon de Medinilla	
Farallon de Pajaros	
Guam	IKONOS
Guguan	
Maug	IKONOS
Marpi	
Pagan	
Rota	WV-2
Saipan	IKONOS
Sarigan	
Tatsumi	
Tinian	IKONOS

American Samoa	Derived Bathymetry
Ofu & Olosega	IKONOS
Rose	IKONOS
South Bank	
Swains	WV-2
Tau	IKONOS
Tutuila	IKONOS

MHI	Derived Bathymetry
Hawaii	
Kaula	
Kauai	
Lanai	
Lehua	
Maui	
Molokini	
Molokai	
Niihau	WV-2
Oahu	
Kahoolawe	

NWHI	Derived Bathymetry
French Frigate	IKONOS
Gardner	
Kure	IKONOS
Laysan	IKONOS
Lisianski	IKONOS
Maro	IKONOS
Midway	IKONOS
Necker	IKONOS
Nihoa	
Pearl & Hermes	IKONOS

PRIA's	Derived Bathymetry
Baker	
Howland	
Jarvis	
Johnston	IKONOS
Kingman	IKONOS
Palmyra	IKONOS
Wake	

The U.S. Pacific Island Region, showing the distribution and availability of shallow-water bathymetry derived from IKONOS, WV-2 multispectral satellite imagery, and LiDAR data.